

A Photophysical and Electrochemical Investigation on a Phenylacetylene Macrocycle Containing Two 2,2'-Bipyridine Units, Its Protonated Forms, and Ru^{II} and Os^{II} Complexes

Margherita Venturi,^{*,[a]} Filippo Marchioni,^[a] Vincenzo Balzani,^[a] Dorina M. Opris,^[b] Oliver Henze,^[b] and A. Dieter Schlüter^[b]

Keywords: Electrochemistry / Luminescence / Macrocycles / Osmium / Ruthenium

The phenylacetylene macrocycle **1**, which incorporates two 2,2'-bipyridine (bpy) chelating units in opposite sites in its shape-persistent structure, shows an intense absorption band in the UV spectral region ($\lambda_{\text{max}} = 305 \text{ nm}$, $\epsilon_{\text{max}} = 118000 \text{ M}^{-1}\text{cm}^{-1}$) and a very strong fluorescence band in dichloromethane solution ($\lambda_{\text{max}} = 381 \text{ nm}$, $\tau = 0.8 \text{ ns}$, $\Phi = 0.9$). Upon titration with trifluoromethanesulfonic acid, the two bpy units are independently protonated with formation of a $[\text{1.2H}]^{2+}$ species that shows a new absorption band with $\lambda_{\text{max}} = 355 \text{ nm}$ ($\epsilon_{\text{max}} = 42000 \text{ M}^{-1}\text{cm}^{-1}$) and a weak fluorescence ($\lambda_{\text{max}} = 520 \text{ nm}$). The dinuclear $[(\text{bpy})_2\text{Ru}(\text{1})\text{Ru}(\text{bpy})_2]^{4+}$ and $[(\text{bpy})_2\text{Os}(\text{1})\text{Os}(\text{bpy})_2]^{4+}$ complexes do not show any ligand-centred emission and exhibit absorption and emission bands in the visible region $\{[(\text{bpy})_2\text{Ru}(\text{1})\text{Ru}(\text{bpy})_2]^{4+}$, absorption: $\lambda_{\text{max}} = 453 \text{ nm}$, $\epsilon_{\text{max}} = 19000 \text{ M}^{-1}\text{cm}^{-1}$; emission: $\lambda_{\text{max}} = 625 \text{ nm}$, $\tau = 792 \text{ ns}$, $\Phi = 0.05$; $[(\text{bpy})_2\text{Os}(\text{1})\text{Os}(\text{bpy})_2]^{4+}$ absorption: $\lambda_{\text{max}} = 488 \text{ nm}$, $\epsilon_{\text{max}} = 15500 \text{ M}^{-1}\text{cm}^{-1}$; emission: $\lambda_{\text{max}} = 740 \text{ nm}$, $\tau = 59 \text{ ns}$, $\Phi = 0.003\}$. The photophysical behaviour

of the macrocyclic ligand **1** and the dinuclear complexes at 77 K has also been investigated. The electrochemical properties of **1**, the model compound ligand **3** and bpy ligand were investigated in purified tetrahydrofuran under vacuum conditions. The electrochemical behaviour of the dinuclear complexes was studied in argon-purged dichloromethane and compared with that of the model compounds $[\text{Ru}(\text{bpy})_2(\text{3})]^{2+}$, $[\text{Ru}(\text{bpy})_3]^{2+}$, and $[\text{Os}(\text{bpy})_3]^{2+}$. In the dinuclear complexes the two metal centres and the two 2,2'-bipyridine units of macrocycle **1** behave independently, as shown by the reversible bielectronic processes observed on oxidation and reduction. Both **1** and its dinuclear complexes contain reactive substituents and can therefore be used as starting components for the construction of photo- and redox-active supramolecular species.

(© Wiley-VCH Verlag GmbH & Co. KGaA, 69451 Weinheim, Germany, 2003)

Introduction

Much attention is currently being devoted to the synthesis and properties of shape-persistent macrocycles.^[1] Such compounds are interesting for a variety of reasons, including the formation of columnar stacks^[2] potentially capable of performing as membrane nanopores. Particularly interesting are shape-persistent macrocycles incorporating coordination units such as 2,2'-bipyridines (bpy). *endo*-Cyclic metal-ion coordination may be exploited to generate nanowires,^[3] whereas *exo*-cyclic coordination can be used

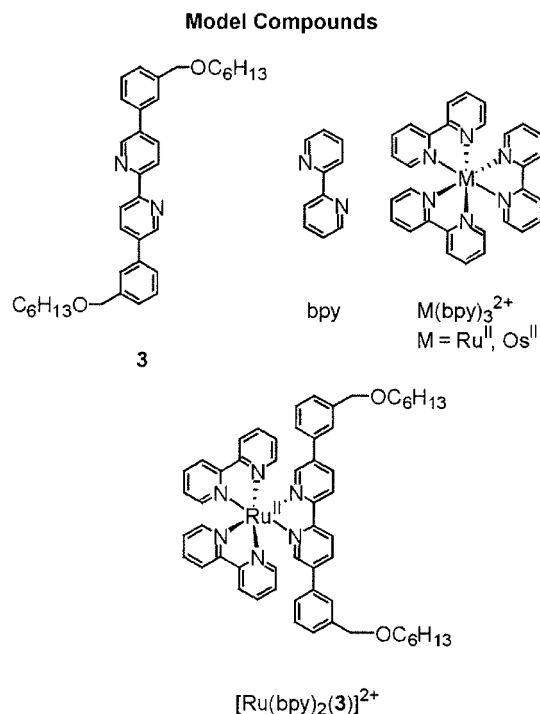
to construct large arrays of polynuclear metal complexes.^[4] Shape-persistent macrocycles with reactive substituents may also be linked to other units to yield multicomponent, hierarchical structures.

In the past few years it has been shown that suitably designed molecular and supramolecular species can perform as nanoscale devices and machines.^[5] An important role in this regard is played by molecular components that respond to external stimuli such as photons, electrons, or protons. Shape-persistent macrocycles exhibiting properties modifiable by photochemical, electrochemical, or acid/base inputs could play important roles in the development of molecular-level devices and machines.

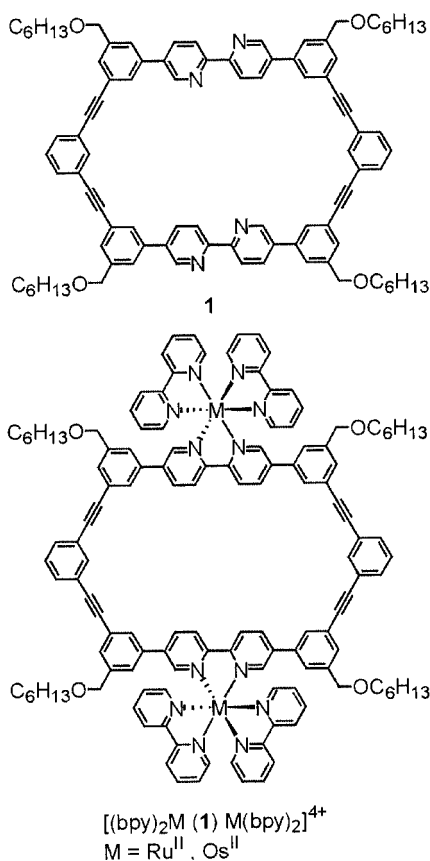
This paper describes an investigation of the photophysical, electrochemical and acid/base properties of the shape-persistent macrocycle **1** and its dinuclear $[(\text{bpy})_2\text{Ru}(\text{1})\text{Ru}(\text{bpy})_2]^{4+}$ and $[(\text{bpy})_2\text{Os}(\text{1})\text{Os}(\text{bpy})_2]^{4+}$ complexes. For a conclusive interpretation of the results, model compounds were also investigated (Scheme 1).

^[a] Dipartimento di Chimica "G. Ciamician", Università di Bologna, Via Selmi 2, 40126 Bologna, Italy
Fax: (internat.) +39-051-2099456
E-mail: mventuri@ciam.unibo.it

^[b] Freie Universität Berlin, Institut für Chemie Takustrasse 3, 14195 Berlin, Germany
Fax: (internat.) +49-(0)30-83853357
E-mail: adschlue@chemie.fu-berlin.de



Scheme 1. Structures of model compounds used



Results and Discussion

Synthesis

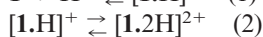
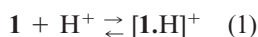
Compound **1** and its dinuclear Ru complex $[(bpy)_2Ru(1)-Ru(bpy)_2]^{4+}$ were synthesized as described in the literature.^[4,6] The synthesis of the corresponding Os complex will be reported elsewhere.^[7] Model compound **3** was prepared from the bpy derivative **2**^[6] by iodo/lithium exchange with butyllithium and subsequent aqueous workup (Scheme 2). Standard complexation of **3** with $[Ru(bpy)_2Cl_2]$ afforded $[Ru(bpy)_2(3)]^{2+}$.

Photophysical Properties

Compound **1** is soluble in methanol, dichloromethane, and tetrahydrofuran. A dichloromethane solution containing 4×10^{-6} M **1** shows a structured absorption band in the UV region with $\lambda_{max} = 305$ nm ($\epsilon_{max} = 118000$ M⁻¹cm⁻¹, Figure 1, Table 1) and an extremely intense fluorescence band with $\lambda_{max} = 381$ nm (Figure 2), $\tau = 0.8$ ns, and $\Phi = 0.9$ (Table 1). Because of the high molar absorption coefficient and the very high fluorescence quantum yield, emission can clearly be seen even for solutions of nanomolar concentrations. In a rigid butyronitrile matrix at 77 K (Table 1), the emission band is slightly blue-shifted ($\lambda_{max} = 375$ nm) and the emission lifetime is slightly increased (1.0 ns).

When a 4×10^{-6} M dichloromethane solution of **1** was titrated with trifluoromethanesulfonic acid, strong spectral changes were observed. A decrease in the intensity of the 305 nm absorption band was accompanied by the formation of a new band with $\lambda_{max} = 355$ nm and $\epsilon_{max} = 42000$ M⁻¹cm⁻¹ (Figure 1, Table 1). In the fluorescence spectrum, the disappearance of the intense band ($\lambda_{max} = 381$ nm) was accompanied by the appearance of a broad and weak band with $\lambda_{max} = 520$ nm (Figure 2, Table 1). The protonation reaction is fully reversible upon addition of tributylamine. Interestingly, the change in the fluorescence intensity at 381 nm (excitation in the isosbestic point at 340 nm) on addition of acid did not parallel the changes in absorbance (Figure 2, inset). For example, a 50% change in the fluorescence intensity plot corresponds to a 34% change in the absorbance plot. These results can be accounted for by assuming that, when one of the macrocycle's bpy units is protonated, the fluorescence of the unprotonated unit of the same macrocycle is quenched by the protonated one, since the latter lies at lower energy. Similar behaviour has been observed upon titration of equivalent fluorescent units in dendrimers^[8] and other supramolecular species.^[9]

The absorption and fluorescence titration profiles were fitted with the aid of the global analysis package SPEC-FIT^[10] according to the following protonation steps:



Both the absorption and fluorescence data were satisfactorily fitted by the values of $\log K_1 = 8.2 \pm 0.5$ and $\log K_2 = 7.3 \pm 0.4$ for the constants of the two protonation

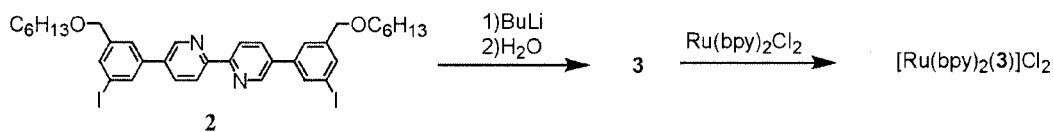
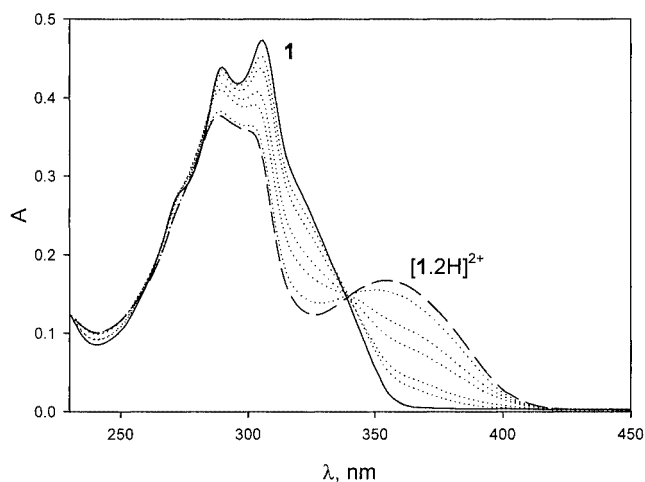
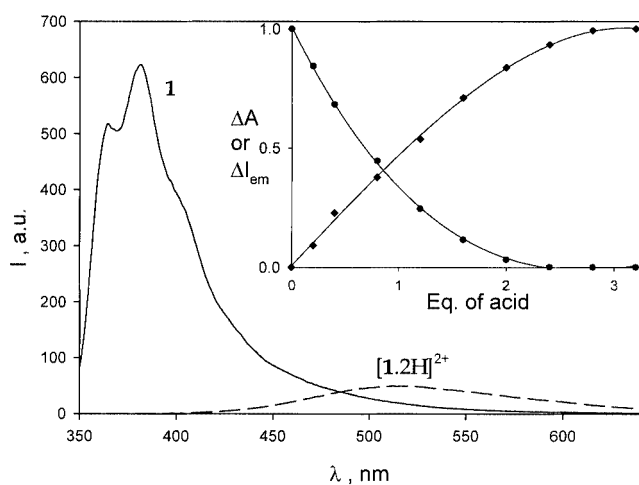
Scheme 2. Synthetic route to ligand **3** and $[\text{Ru}(\text{bpy})_2(\mathbf{3})]^{2+}$ complex

Table 1. Absorption and emission properties

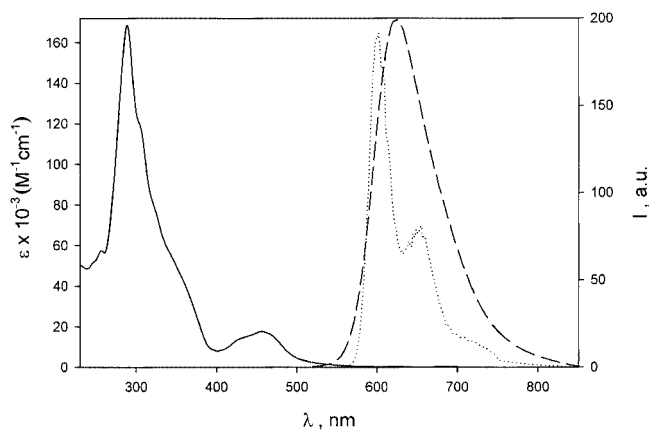
Ligand/Complex	Absorption ^[a] 298 K		298 K ^[a]		Luminescence		77 K
	λ_{max} , nm	ϵ ($\text{M}^{-1} \text{cm}^{-1}$)	λ_{max} , nm	τ , ns	Φ	λ_{max} , nm	τ , μs
1	305	118000	381	0.8	0.9	375 ^[b]	0.001 ^[b]
$[\mathbf{1.2H}]^{2+}$	355	42000	520				
$[(\text{bpy})_2\text{Ru}(\mathbf{1})\text{Ru}(\text{bpy})_2]^{4+}$	453	19000	625	792	0.05	600 ^[c]	5.14 ^[c]
$[(\text{bpy})_2\text{Os}(\mathbf{1})\text{Os}(\text{bpy})_2]^{4+}$	488	15500	740	59	0.003	735 ^[c]	0.97 ^[c]

^[a] Dichloromethane solution. ^[b] Butyronitrile rigid matrix. ^[c] Dichloromethane/methanol (1:1, v/v) rigid matrix.

Figure 1. Absorption spectral changes observed during the titration of **1** with trifluoromethanesulfonic acid in dichloromethane solution (optical path length: 1 cm)Figure 2. Emission spectra of **1** and $[\mathbf{1.2H}]^{2+}$ in dichloromethane solution; inset: normalised absorption (●, $\lambda = 380$ nm) and emission (○, $\lambda = 381$ nm) changes during the titration with trifluoromethanesulfonic acid

steps. These data indicate that the two bpy units of ligand **1** undergo practically independent protonation, as would be expected because of their relative large separation.^[6] It is interesting to note that in the case of the bpy ligand in dichloromethane solution we have found a value of $\log K = 8.3 \pm 0.7$ ^[11] for the constant of the first protonation step, which is in full agreement with the data obtained for ligand **1**.

In dichloromethane solution, the $[(\text{bpy})_2\text{Ru}(\mathbf{1})\text{Ru}(\text{bpy})_2]^{4+}$ complex exhibits absorption ($\lambda_{\text{max}} = 453$ nm, $\epsilon_{\text{max}} = 19000 \text{ M}^{-1}\text{cm}^{-1}$) and emission bands ($\lambda_{\text{max}} = 625$ nm, $\tau = 792$ ns, $\Phi = 0.05$) in the visible region (Figure 3, Table 1). These bands can be straightforwardly assigned to spin-allowed and spin-forbidden metal-to-ligand-charge-transfer (MLCT) excited states, respectively, characteristic of Ru^{II} polypyridine complexes.^[12] In a rigid methanol/dichloromethane (1:1, v/v) matrix at 77 K (Table 1), $[(\text{bpy})_2\text{Ru}(\mathbf{1})\text{Ru}(\text{bpy})_2]^{4+}$ shows a structured emission band with $\lambda_{\text{max}} = 600$ nm (Figure 3) and $\tau = 5.14 \mu\text{s}$, again typical of Ru^{II} polypyridine complexes.^[12] The mononuclear complex $[\text{Ru}(\text{bpy})_2(\mathbf{3})]^{2+}$ (Scheme 1) shows similar spectro-

Figure 3. Absorption (dichloromethane solution; full line) and emission (dichloromethane solution at 298 K, dashed line; methanol/dichloromethane rigid matrix at 77 K, dotted line) spectra of the $[(\text{bpy})_2\text{Ru}(\mathbf{1})\text{Ru}(\text{bpy})_2]^{4+}$ complex

scopic behaviour in dichloromethane solution: (i) the MLCT absorption band shows a maximum at 456 nm with $\epsilon_{\max} = 10000 \text{ M}^{-1}\text{cm}^{-1}$, which is practically one half of that of $[(\text{bpy})_2\text{Ru}(\mathbf{1})\text{Ru}(\text{bpy})_2]^{4+}$, and (ii) the emission properties at room temperature ($\lambda_{\max} = 607 \text{ nm}$, $\tau = 630 \text{ ns}$, $\Phi = 0.07$) and at 77 K ($\lambda_{\max} = 591 \text{ nm}$ and $\tau = 5.7 \mu\text{s}$) are almost the same as those of the dinuclear complex. It can also be seen that both compounds behave quite similarly to $[\text{Ru}(\text{bpy})_3]^{2+}$.^[12a]

In dichloromethane solution, the $[(\text{bpy})_2\text{Os}(\mathbf{1})\text{Os}(\text{bpy})_2]^{4+}$ complex exhibits absorption ($\lambda_{\max} = 488 \text{ nm}$, $\epsilon_{\max} = 15500 \text{ M}^{-1}\text{cm}^{-1}$) and emission bands ($\lambda_{\max} = 740 \text{ nm}$, $\tau = 59 \text{ ns}$, $\Phi = 0.003$) in the visible region (Figure 4, Table 1). These bands can be straightforwardly assigned to spin-allowed and spin-forbidden MLCT excited states, respectively, characteristic of the Os^{II} polypyridine complexes.^[13] In a rigid methanol/dichloromethane (1:1, v/v) matrix at 77 K (Table 1), $[(\text{bpy})_2\text{Os}(\mathbf{1})\text{Os}(\text{bpy})_2]^{4+}$ shows a structured emission band with $\lambda_{\max} = 735 \text{ nm}$ (Figure 4) and $\tau = 0.97 \mu\text{s}$, again typical of Os^{II} polypyridine complexes.^[13]

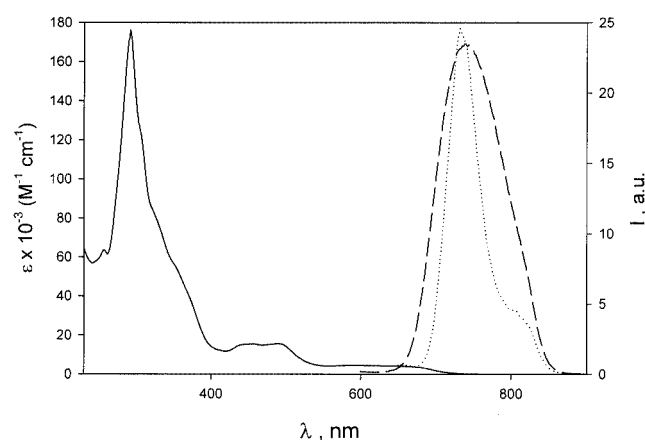


Figure 4. Absorption (dichloromethane solution; full line) and emission (dichloromethane solution at 298 K, dashed line; methanol/dichloromethane rigid matrix at 77 K, dotted line) spectra of the $[(\text{bpy})_2\text{Os}(\mathbf{1})\text{Os}(\text{bpy})_2]^{4+}$ complex

Electrochemical Properties

The electrochemical properties of compound **1** were investigated in purified tetrahydrofuran under vacuum conditions (see Exp. Sect.). In the accessible potential window (+1/−3 V vs. SCE), compound **1** undergoes three reversible bielectronic reduction processes, at −1.76, −1.94, and −2.07 V vs. SCE, a fourth irreversible reduction process at −2.36 V vs. SCE, and no oxidation processes (Table 2). A comparison with the data obtained under the same conditions for ligand **3**, which can be regarded as a model compound for the bpy units of **1**, and bpy ligand (Table 2) shows that: (i) the macrocyclic ligand **1** is easier to reduce than the other two ligands, and (ii) the two bpy units of **1** are equivalent and behave independently, as indicated by the fact that they are simultaneously reduced at the same potential value.

In the electrochemical experiments performed in argon-purged dichloromethane solution, $[(\text{bpy})_2\text{Ru}(\mathbf{1})\text{Ru}(\text{bpy})_2]^{4+}$ undergoes a reversible bielectronic oxidation at +1.44 V vs. SCE (Figure 5, Table 2), which can be assigned to the concomitant oxidation of the two metal centres.^[12b] This result shows that the two metal centres of $[(\text{bpy})_2\text{Ru}(\mathbf{1})\text{Ru}(\text{bpy})_2]^{4+}$ are equivalent and do not interact with one another. The potential value at which the two Ru ions are simultaneously oxidized is very similar to that observed for the metal oxidation in $[\text{Ru}(\text{bpy})_2(\mathbf{3})]^{2+}$ and $[\text{Ru}(\text{bpy})_3]^{2+}$ (Figure 6, Table 2). On reduction, two reversible bielectronic processes are observed in the accessible potential window, which can be attributed to the reduction of the ligands (Figure 5, Table 2).^[12] By comparison with the data obtained for $[\text{Ru}(\text{bpy})_2(\mathbf{3})]^{2+}$ and $[\text{Ru}(\text{bpy})_3]^{2+}$ (Figure 6, Table 2), these processes can be easily assigned as follows: (i) the first process at −1.13 V vs. SCE concerns the simultaneous reduction of the two bpy units of the ligand **1**, considering that such a ligand is easier to reduce than the bpy ligand, and (ii) the second process at −1.43 V vs. SCE involves two bpy ligands, one for each $\text{Ru}(\text{bpy})_2$ moiety, which are reduced simultaneously at the same potential. This process occurs at a potential value: (a) more negative than that of the first reduction of $[\text{Ru}(\text{bpy})_3]^{2+}$, because in

Table 2. Redox potentials of macrocycle **1**, $[(\text{bpy})_2\text{Ru}(\mathbf{1})\text{Ru}(\text{bpy})_2]^{4+}$, $[(\text{bpy})_2\text{Os}(\mathbf{1})\text{Os}(\text{bpy})_2]^{4+}$, and some model compounds^[a]

Ligand/Complex	Ligand-centred reduction $E_{1/2}$ (ΔV) ^[b] [n] ^[c]				Metal-centred oxidation $E_{1/2}$ (ΔV) ^[b] [n] ^[c]
1 ^[d]	−2.36 ^[e]	−2.07 (60) [2]	−1.94 (60) [2]	−1.76 (66) [2]	
$[(\text{bpy})_2\text{Ru}(\mathbf{1})\text{Ru}(\text{bpy})_2]^{4+}$			−1.43 (80) [2]	−1.13 (70) [2]	+1.44 (80) [2]
$[(\text{bpy})_2\text{Os}(\mathbf{1})\text{Os}(\text{bpy})_2]^{4+}$			−1.35 (105) [2]	−1.06 (100) [2]	+1.03 (90) [2]
3 ^[d]		−2.60 ^[e]	−2.13 (90) [1]	−1.85 (80) [1]	
bpy ^[d]			−2.69 ^[e]	−2.18 (100) [1]	
$[\text{Ru}(\text{bpy})_2(\mathbf{3})]^{2+}$			−1.43 (70) [1]	−1.12 (60) [1]	+1.45 (80) [1]
$[\text{Ru}(\text{bpy})_3]^{2+}$			−1.50 (90) [1]	−1.24 (70) [1]	+1.43 (78) [1]
$[\text{Os}(\text{bpy})_3]^{2+}$			−1.35 (100) [1]	−1.06 (90) [1]	+1.03 (90) [1]

^[a] Room temperature argon-purged dichloromethane solution, unless otherwise noted; half-wave potential values in V vs. SCE; tetrabutylammonium hexafluorophosphate as supporting electrolyte, glassy carbon as working electrode. ^[b] Average value of $|E_a - E_c|$ in mV.

^[c] Number of the exchanged electrons. ^[d] Purified tetrahydrofuran under vacuum conditions. ^[e] Irreversible process; potential value estimated by the DPV peak.

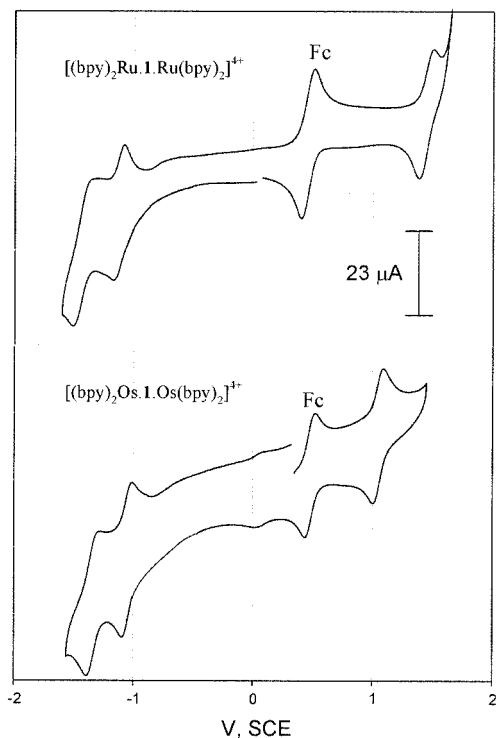


Figure 5. Cyclic voltammograms obtained for the dinuclear complexes (argon-purged dichloromethane; complex concentration 1×10^{-3} M; glassy carbon as working electrode, scan rate of 200 mV/s); Fc indicates the wave of the ferrocene added as internal reference

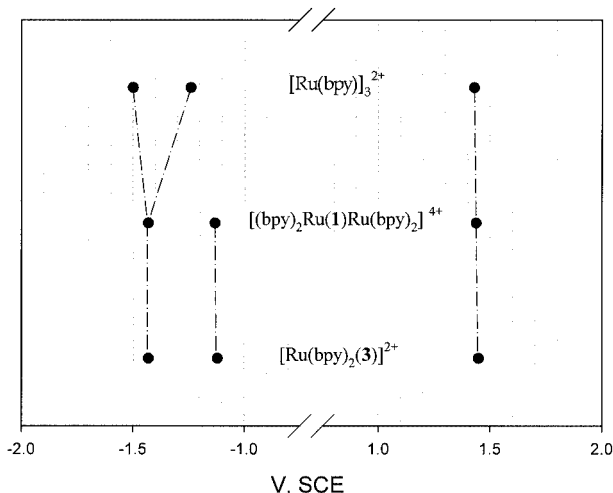


Figure 6. Correlation diagram for the reduction and oxidation processes (argon-purged dichloromethane) of $[(bpy)_2Ru(1)Ru(bpy)_2]^{4+}$ and the model compounds $[Ru(bpy)_2(3)]^{2+}$ and $[Ru(bpy)_3]^{2+}$

the dinuclear complex the bpy ligand reduction is preceded by the reduction of the bpy units of ligand **1**, and (b) less negative than that of the second reduction of $[Ru(bpy)_3]^{2+}$ because of the greater delocalization of the charges introduced by replacement of one bpy with the ligand **1**. The same considerations can be used to compare the behaviour of $[Ru(bpy)_2(3)]^{2+}$ and $[Ru(bpy)_3]^{2+}$.

In the electrochemical experiments performed in argon-purged dichloromethane solution, $[(bpy)_2Os(1)Os(bpy)_2]^{4+}$

undergoes a reversible bielectronic oxidation at +1.03 V vs. SCE (Figure 5, Table 2), which can be assigned to the concomitant oxidation of the two metal centres.^[12b] As already discussed for $[(bpy)_2Ru(1)Ru(bpy)_2]^{4+}$, this result shows that the two Os centres are equivalent and do not interact with one another. The potential value at which the two Os ions are simultaneously oxidized is identical to that obtained for the metal oxidation in $[Os(bpy)_3]^{2+}$ (Table 2). On reduction, two reversible bielectronic processes are observed in the accessible potential window. Consistently with the dinuclear Ru-based complex discussed above, the first process at -1.06 V vs. SCE can be assigned to the reduction of ligand **1**, while the second process at -1.35 V vs. SCE concerns the simultaneous reduction of two bpy ligands, one for each $Os(bpy)_2$ moiety. The fact that these processes occur at the same potential values as observed for $[Os(bpy)_3]^{2+}$ (Table 2) can be explained by considering that the Os ion to be capable of delocalising the introduced charges better than the Ru ion.^[14]

Conclusions

The shape-persistent macrocycle **1** exhibits very interesting photophysical properties. In particular, it shows a fluorescence band with a quantum yield of almost unity. Upon protonation, strong changes are observed in its absorption and emission properties. In the monoprotonated species, the strong fluorescence of the unprotonated bpy unit is quenched by the protonated one. Macrocycle **1** is also a bis(chelating) ligand, which reacts with $[Ru(bpy)_2Cl_2]$ and $[Os(bpy)_2Cl_2]$ to give the dinuclear $[(bpy)_2Ru(1)Ru(bpy)_2]^{4+}$ and $[(bpy)_2Os(1)Os(bpy)_2]^{4+}$ complexes, respectively. These dinuclear complexes do not show any ligand-centred emission and exhibit absorption and emission bands in the visible region. The electrochemical investigation has indicated that in the dinuclear complexes the two metal centres and the two bpy units of the macrocycle **1** behave independently as shown by the reversible bielectronic processes observed on oxidation and reduction, respectively. Both **1** and its dinuclear complexes can be functionalized with reactive substituents and can therefore be used as components of larger supramolecular species.

Experimental Section

Syntheses: Compounds **1**, **2** and $[(bpy)_2Ru(1)Ru(bpy)_2]^{4+}$ were prepared and characterized as previously reported.^[4,6] All other chemicals were purchased from Aldrich or Fluka and used without further purification. Melting points: Büchi SMP 510 (open capillaries, uncorrected values). NMR: Bruker AC 250, AM 270, 1H NMR referenced to $CDCl_3$ at $\delta = 7.24$ ppm, ^{13}C NMR referenced to $CDCl_3$ at $\delta = 77.00$ ppm. MS: Perkin–Elmer Varian MAT 711, electron-impact (EI) mode. Elemental analyses: Perkin–Elmer EA 240. Column chromatography: Merck silica gel 60, 0.040–0.063 mm (230–400 mesh).

Compound 3: A solution of BuLi in hexane (1.6 M, 0.7 mL) was added dropwise at -78 °C to a stirred suspension of the diiodo

compound **2** (0.4 g, 0.51 mmol) in dry THF (15 mL). After the mixture had been kept for 3 h at -78°C , water was added and the reaction mixture was warmed to room temp. The solvent was removed, the residue was dissolved in dichloromethane (10 mL), and water (5 mL) was added. The phases were separated. The aqueous one was extracted twice with dichloromethane (5 mL each) and the combined organic phases were dried with MgSO_4 . After filtration and evaporation of the solvent, the compound was purified by column chromatography through silica gel with hexane/ethyl acetate (7:1) as eluent to provide compound **3** (0.14 g, 50%) as a white solid. R_f (hexane/ethyl acetate, 7:1) = 0.16. ^1H NMR (CDCl_3): δ = 0.88 (t, 6 H, CH_3), 1.24–1.40 (m, 12 H, $\gamma,\delta,\epsilon\text{-CH}_2$) 1.68 (m, 4 H, $\beta\text{-CH}_2$), 3.50 (t, 4 H, $\alpha\text{-CH}_2$), 4.50 (s, 4 H, benzyl- CH_2), 7.36 (d, 2 H, phenyl-H), 7.46 (dd, 2 H, phenyl-H), 7.56 (d, 2 H, phenyl-H), 7.64 (s, 2 H, phenyl-H), 8.04 (dd, 3J = 8, 4J = 2 Hz, 2 H, py-H), 8.50 (d, 3J = 8 Hz, 2 H, py-H), 8.92 (s, 2 H, py-H) ppm. ^{13}C NMR (CDCl_3 , 63 MHz): δ = 13.98, 22.56, 25.85, 29.70, 31.64, 70.77, 72.61, 120.97, 126.12, 127.35, 129.10, 135.27, 136.39, 137.60, 139.78, 147.56, 154.42 ppm. MS: m/z (%) = 536 (100), 451 (49), 435.9 (61). HRMS: m/z calcd. for $\text{C}_{36}\text{H}_{44}\text{N}_2\text{O}_2$ 536.3403; found 536.3453.

[Ru(bpy)₂(3**)]²⁺**: A stirred solution of ligand **3** (72 mg, 0.134 mmol) and $[\text{Ru}(\text{bpy})_2\text{Cl}_2]\cdot 2\text{H}_2\text{O}$ (70 mg, 0.134 mmol) in ethanol (2.5 mL) and water (0.8 mL) was heated at reflux under nitrogen for 24 h. The solvent was removed and the residual orange material was purified by column chromatography through silica gel (methanol/2 M NH_4Cl /nitromethane, 7:2:1). The combined organic fractions were diluted with dichloromethane, the organic phases were separated, and the solvent was removed. The orange residue was then dissolved in methanol (1 mL) and added to a solution of NH_4PF_6 (134 mg) in 1 mL water. The precipitate was filtered and washed several times with water to give $[\text{Ru}(\text{bpy})_2(\textbf{3})]^{2+}$ (0.14 g, 89%) as an orange solid. ^1H NMR (CDCl_3): δ = 0.82 (t, 6 H, CH_3), 1.21 (m, 12 H, $\gamma,\delta,\epsilon\text{-CH}_2$) 1.54 (m, 4 H, $\beta\text{-CH}_2$), 3.42 (t, 4 H, $\alpha\text{-CH}_2$), 4.42 (s, 4 H, benzyl- CH_2), 7.12 (t, 2 H, phenyl-H), 7.30 (m, 6 H, phenyl-H), 7.42 (t, 4 H, phenyl-H), 7.65 (s, 2 H, py-H), 7.72 (d, 3J = 8 Hz, 2 H, py-H), 7.80 (d, 3J = 8 Hz, 2 H, py-H), 7.90 (m, 4 H, py-H), 8.15 (d, 3J = 8 Hz, 2 H, py-H), 8.42 (d, 3J = 8 Hz, 4 H, py-H), 8.53 (d, 3J = 8 Hz, 2 H, py-H) ppm. ^{13}C NMR (CDCl_3 , 63 MHz): δ = 13.81, 22.38, 25.61, 29.49, 31.45, 70.77, 71.99, 116.35, 124.00, 124.28, 125.96, 127.93, 128.26, 128.77, 129.54, 134.30, 136.10, 137.85, 138.09, 140.30, 140.44, 148.113.81, 22.38, 25.61, 29.49, 31.45, 70.77, 71.99, 116.35, 124.00, 124.28, 125.96, 127.93, 128.26, 128.77, 129.54, 134.30, 136.10, 137.85, 138.09, 140.30, 140.44, 148.15, 151.29, 151.50, 153.44, 154.85, 156.19, 156.61 ppm. MALDI-TOF: m/z = 1095.4 [$\text{M} - \text{PF}_6$], 950.4 [$\text{M} - 2\text{PF}_6$], 794.3 [$\text{M} - 2\text{PF}_6 - \text{bipy}$]. $\text{C}_{56}\text{H}_{60}\text{F}_{12}\text{N}_6\text{O}_2\text{P}_2\text{Ru}$ (1240.1): calcd. C 54.24, H 4.88, N 6.78; found C 53.90, H 4.69, N 6.51.

Photophysics and Electrochemistry: The equipment used for investigation of absorption spectra and luminescence properties (in fluid solution and in rigid matrix) has been described previously.^[15] Anthracene in air-equilibrated ethanol (Φ = 0.21)^[16] and $[\text{Ru}(\text{bpy})_3]^{2+}$ in air-equilibrated aqueous solution (Φ = 0.028)^[17] were used as standards for evaluation of the luminescence quantum yield of **1** and the dinuclear complexes, respectively. Unless otherwise stated, air-equilibrated solutions were used.

The electrochemical investigation of ligands **1**, **3**, and bpy was carried out by use of a cell of airtight design with high-vacuum glass stopcocks fitted with Teflon O-rings. A weighed amount of the investigated compounds was introduced into the electrochemical cell together with the desired amount of supporting electrolyte. The cell was evacuated and kept under vacuum (typical pressure: $2 \times$

10^{-5} mbar) for at least 3 hours. Tetrahydrofuran was then vapour-transferred from a Schlenk vessel in which it was stored in the presence of sodium anthracenide prepared according to the procedure reported in the literature.^[18] The working electrode was a glassy carbon (0.14 cm^2) electrode, the counter-electrode was a platinum spiral, and the quasi-reference electrode was a silver spiral. The equipment used for investigation of the electrochemical behaviour of the complexes in argon-purged Hi-dry dichloromethane has been described previously.^[15] In all the electrochemical experiments, the compound concentration was in the $1 \times 10^{-3} - 5 \times 10^{-4}$ M range, and tetrabutylammonium hexafluorophosphate with a concentration a hundred times higher was added as supporting electrolyte. Ferrocene was used as internal reference ($E_{1/2}$ = +0.46 V vs. SCE in dichloromethane; $E_{1/2}$ = +0.57 V vs. SCE in tetrahydrofuran).^[19] Cyclic voltammetric (CV) and differential pulse voltammetric (DPV) experiments were used to determine the electrochemical properties of all the investigated compounds. CV experiments were obtained with sweep rates in the 0.02–1.0 V/s range; the DPV experiments were performed with a scan rate of 20 or 4 mV/s (pulse height 75 and 10 mV, respectively) and a duration of 40 ms. The reversibility of the observed processes was established by use of the criteria: (i) separation of 60 mV between cathodic and anodic peaks, (ii) the close to unity ratio of the intensities of the cathodic and anodic currents, and (iii) the constancy of the peak potential on changing sweep rate in the cyclic voltammograms. The same half-wave potential values were obtained from the DPV peaks and from an average of the cathodic and anodic CV peaks, as expected for reversible processes. For irreversible processes the potential values were estimated from the DPV peaks. The number of the exchanged electrons for reversible processes involving macrocycle **1** and ligand **3** was measured by comparison of the current intensity of the CV waves and the area of the DPV peaks with those found for the first reversible monoelectronic process of the bpy ligand, after correction for differences in concentrations and diffusion coefficients.^[20] The number of the exchanged electrons for the processes involving the complexes was obtained by the same procedure by use of the reversible monoelectronic processes exhibited by $[\text{Ru}(\text{bpy})_3]^{2+}$ as reference.

Experimental errors: molar absorption coefficients, $\pm 5\%$; luminescence quantum yield, $\pm 10\%$; luminescence lifetime, $\pm 5\%$; redox potentials, 10 mV and 20 mV for reversible and irreversible processes, respectively.

Acknowledgments

This research was supported by the MIUR (Supramolecular Devices Project), the University of Bologna (Funds for Selected Topics) and the Deutsche Forschungsgemeinschaft (Sfb, 448, TP A1), which is gratefully acknowledged.

- [1] [1a] S. Höger, *J. Polym. Sci. Polym. Chem.* **1999**, *37*, 2685–2698.
[1b] C. Grave, A. D. Schlüter, *Eur. J. Org. Chem.* **2002**, 3075–3098. [1c] D. Zhao, J. S. Moore, *Chem. Commun.* **2003**, 807–818.
- [2] D. H. Cobden, *Nature* **2001**, *409*, 32–33.
- [3] L. T. Scott, G. J. DeCicco, G. Reinhardt, *J. Am. Chem. Soc.* **1985**, *107*, 6546–6555.
- [4] O. Henze, D. Lentz, A. Schäfer, P. Franke, A. D. Schlüter, *Chem. Eur. J.* **2002**, *8*, 357–365, and references cited therein.
- [5] [5a] V. Balzani, A. Credi, F. M. Raymo, J. F. Stoddart, *Angew. Chem. Int. Ed.* **2000**, *39*, 3348–3391. [5b] V. Balzani, A. Credi, M. Venturi, *Molecular Devices and Machines – A Journey into the Nanoworld*, Wiley-VCH, Weinheim, **2003**.

- [6] O. Henze, D. Lentz, A. D. Schlüter, *Chem. Eur. J.* **2000**, *6*, 2362–2367.
- [7] D. M. Opris, A. D. Schlüter, unpublished results.
- [8] F. Vögtle, S. Gestermann, C. Kauffmann, P. Cerroni, V. Vicinelli, L. De Cola, V. Balzani, *J. Am. Chem. Soc.* **1999**, *121*, 12161–12166.
- [9] R. Ballardini, V. Balzani, A. Credi, M. T. Gandolfi, F. Hotzyba-Hilbert, J.-M. Lehn, L. Prodi, *J. Am. Chem. Soc.* **1994**, *116*, 5743–5746.
- [10] [10a] R. A. Binstead, *SPECFIT*; Spectrum Software Associates, Chapel Hill, NC, 1996. [10b] H. Gampp, M. Maeder, C. J. Meyer, A. D. Zuberbühler, *Talanta* **1985**, *32*, 257–264.
- [11] Unpublished results obtained in our laboratories.
- [12] [12a] A. Juris, V. Balzani, F. Barigelletti, S. Campagna, P. Belser, A. Von Zelewsky, *Coord. Chem. Rev.* **1988**, *84*, 85–277. [12b] V. Balzani, A. Juris, M. Venturi, S. Campagna, S. Serroni, *Chem. Rev.* **1996**, *96*, 759–834.
- [13] K. Kalyanasundaram, *Photochemistry of Polypyridine and Porphyrin Complexes*, Academic Press, London, **1992**.
- [14] G. Giuffrida, S. Campagna, *Coord. Chem. Rev.* **1994**, *135/136*, 517–531.
- [15] D. B. Amabilino, M. Asakawa, P. R. Ashton, R. Ballardini, V. Balzani, M. Belohradsky, A. Credi, M. Higuchi, F. M. Raymo, T. Shimizu, J. F. Stoddart, M. Venturi, K. Yase, *New J. Chem.* **1998**, 959–972.
- [16] W. H. Melhuish, *J. Phys. Chem.* **1961**, *65*, 229–235.
- [17] K. Nakamaru, *Bull. Chem. Soc. Jpn.* **1982**, *55*, 2697–2705.
- [18] F. Paolucci, M. Carano, P. Ceroni, L. Mottier, S. Roffia, *J. Electrochem. Soc.* **1999**, *146*, 3357–3360.
- [19] D. Dubois, G. Mininot, W. Kutner, M. T. Jones, K. M. Kadish, *J. Phys. Chem.* **1992**, *96*, 7137–7145.
- [20] J. B. Flanagan, S. Margel, A. J. Bard, F. C. Anson, *J. Am. Chem. Soc.* **1978**, *100*, 4248–4253.

Received June 25, 2003